

Self-Capacitance of Inductors

Antonio Massarini and Marian K. Kazimierczuk, *Senior Member, IEEE*

Abstract—A new method for predicting the stray capacitance of inductors is presented. The method is based on an analytical approach and the physical structure of inductors. The inductor winding is partitioned into basic cells—many of which are identical. An expression for the equivalent capacitance of the basic cell is derived. Using this expression, the stray capacitance is found for both single- and multiple-layer coils, including the presence of the core. The method was tested with experimental measurements. The accuracy of the results is good. The derived expressions are useful for designing inductors and can be used for simulation purposes.

Index Terms—Modeling of inductors, self-capacitance.

I. INTRODUCTION

THE UPPER operating frequency of every inductor is limited by its self-capacitance. At high frequencies, the response of inductors and transformers is very different from their ac low-frequency response. Skin and proximity effects cause the winding parasitic resistance to increase with the operating frequency, and the parasitic capacitance of the winding cannot be neglected either. Therefore, an accurate prediction of the response of inductors that operate at frequencies above several hundred kilohertz, such as, for instance, those used in high-frequency switching power converters, is crucial for the design of high-frequency power circuits. Unfortunately, the parasitic capacitances and resistances are distributed parameters, and their values depend on the operating frequency. Therefore, the theoretical prediction of the frequency response of an inductor is a difficult problem.

High-frequency behavior of magnetic components is widely discussed in the literature, but mainly the aspects related to the parasitic ac winding resistances and core losses have been addressed [1]–[6]. Some results concerning the stray capacitance of single- and multiple-layer coils have been presented in [7]–[12]. These publications offer some interesting physical insights, but the results rely on some experimental data.

The purpose of this paper is to present a new method for predicting the stray capacitance of single- or multiple-layer inductors and compare the theoretical and experimental results. The proposed method is based on an analytical approach. It can predict the stray capacitance of an inductor as a function of a few parameters of the geometry and the number of layers.

Manuscript received December 14, 1995; revised September 16, 1996. Recommended by Associate Editor, W. J. Sarjeant.

A. Massarini is with the Department of Electrical Engineering, Wright State University, Dayton, OH 45435 USA, on leave from the Department of Science and Engineering, University of Modena, 41100 Modena, Italy.

M. K. Kazimierczuk is with the Department of Electrical Engineering, Wright State University, Dayton, OH 45435 USA.

Publisher Item Identifier S 0885-8993(97)04976-4.

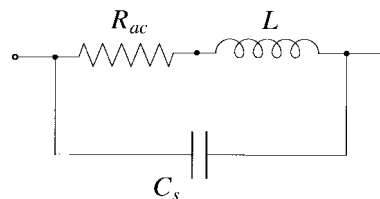


Fig. 1. Equivalent circuit of an inductor.

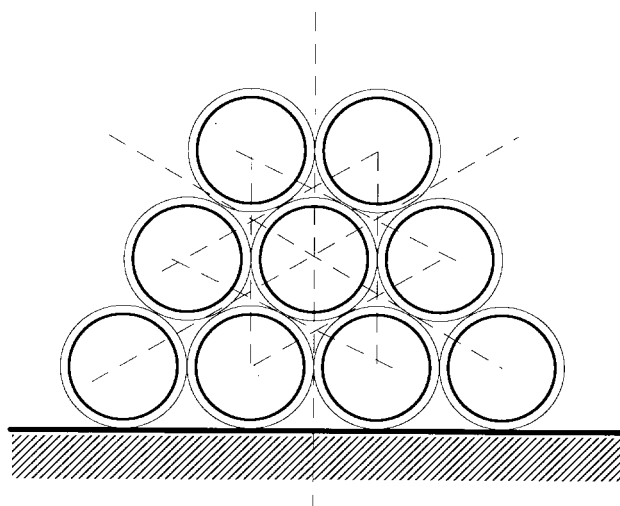


Fig. 2. Cross-sectional view of a three-layer winding.

II. MODEL OF THE PARASITIC CAPACITANCE

Inductor windings have a distributed parasitic capacitance. The distributed capacitance of inductors can be modeled by a lumped capacitance connected between the terminals of the winding, as shown in Fig. 1. The analysis in this paper is performed for inductors made of a uniformly wound single wire, as shown in Fig. 2. The total stray capacitance of inductors consists of the following components:

- 1) the turn-to-turn capacitances between turns of the same layer;
- 2) the turn-to-turn capacitances between turns of adjacent layers;
- 3) the turn-to-core and turn-to-shield capacitances.

The cross-sectional view of a uniformly wound coil consisting of three layers is shown in Fig. 2. The basic cell $ABCD$ related to the turn-to-turn capacitance is shown in Fig. 3. From these figures, we can notice symmetries in the winding geometry. In particular, the lines of the electric field \mathbf{E} that get out from a turn fully surrounded by other conductors go to these conductors. No line can go to infinity if we assume that the conductors of the coil (turns, core, and shield) are

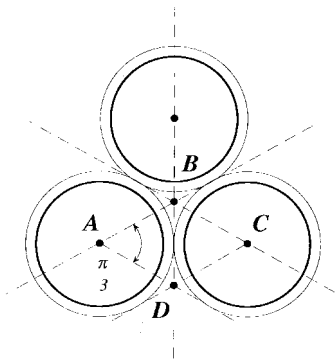


Fig. 3. A basic cell $ABCD$ representing the turn-to-turn capacitance.

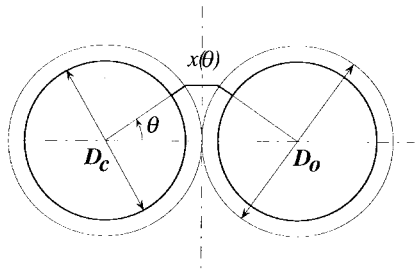


Fig. 4. Assumed path $x(\theta)$ of an electric field line \mathbf{E} at angle θ between two adjacent turns.

close to each other. As a consequence of the geometrical symmetries of the coil, the lines of the electric field must be equally shared between the adjacent conductors. If we consider two adjacent conductors, the elementary capacitance dC between two opposite corresponding elementary surfaces of these conductors dS is given by

$$dC = \epsilon \frac{dS}{x} \quad (1)$$

where $\epsilon = \epsilon_r \epsilon_0$ is the permittivity of the medium and x is the length of a line of the electric field connecting the two opposite elementary surfaces. In the most general case, the length x is not constant, but can be a function of the location of the elementary surface. Therefore, some coordinate system should be selected. For a round conductor, the location of each elementary surface can be described by one angular coordinate θ , as shown in Fig. 4. As a consequence, the elementary capacitance dC also depends on the angular coordinate θ .

III. TURN-TO-TURN CAPACITANCE

A. Structure of the Basic Cell

A basic cell $ABCD$ that forms the turn-to-turn capacitance is shown in Fig. 3. It can be seen that the basic cell is the same for two adjacent turns of the same layer and two adjacent turns of different layers. Therefore, the inner part of the winding can be divided into identical basic cells. Only the cells adjacent to the core and shield differ from the turn-to-turn cells. Yet, as a first-order approximation, we can consider all the basic cells identical. They include a portion of the perimeter of the turn, which corresponds to an angle of $\pi/3$ rad, as shown in Fig. 3. Hence, in order to obtain the turn-to-turn capacitance,

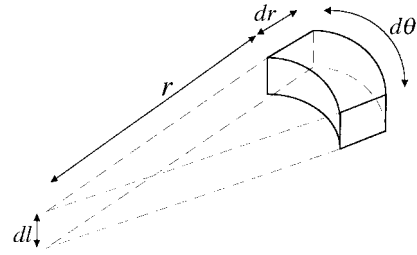


Fig. 5. Elementary cylindrical surface located inside of the insulating coating.

(1) must be integrated over the angle $\pi/3$. This is true for turns fully surrounded by other conductors because of the symmetries, as can be seen from Figs. 2 and 3. As a first-order approximation, the same angle can also be used for turns not completely surrounded. This approximation is equivalent to neglecting the fringing effects.

For the basic cell shown in Fig. 3, three different regions are crossed by the lines of the electric field: two insulating coatings and the air gap between them. The elementary capacitance dC between adjacent turns is, therefore, equivalent to the capacitance of a series combination of three elementary capacitors, each with a uniform dielectric material. The first capacitor is related to the insulating coating of the first turn, the second capacitor is related to the air gap, and the third capacitor is related to the insulating coating of the second turn. The conductor surface can be considered an equipotential one with a good approximation. Therefore, the lines of the electric field must be orthogonal to the conductor surfaces. If the thickness of the insulating coating s is much lower than the outer diameter of the wire, including insulation D_o , we can approximate the paths of the electric field in the insulator by the insulator thickness s , as shown in Fig. 4.

It is more difficult to evaluate the paths of the electric field in the air gap between adjacent turns. The shortest possible paths can be used as a conservative approximation. These paths are given by segments parallel to the line that connects the centerlines of the turns under consideration. One of these segments is depicted in Fig. 4, along with its angular coordinate θ . This approximation is valid for small values of θ , which give the greater contributions to the turn-to-turn capacitance. For increasing values of θ , the error caused by the approximation increases, which leads to somewhat larger than actual capacitances at relatively bigger values of θ . However, the contribution to the turn-to-turn capacitance of the surfaces at increasing values of θ also decreases, and the error becomes negligible.

B. Capacitance of the Insulating Coatings

Let us derive now an expression for the capacitance of the insulating coatings. Fig. 5 shows an elementary cylindrical surface located between the conductor surface and external coating surface. The elementary capacitance related to the cylindrical coating shell is given by

$$dC = \frac{\epsilon_r \epsilon_0 r}{dr} d\theta dl. \quad (2)$$

Integrating this equation for r ranging from the radius of the conductor without the coating r_c to the outer radius of the wire, including coating r_o , and for l from zero to the turn length l_t , one obtains the capacitance of the insulating coating related to an elementary angle $d\theta$:

$$dC_c = \epsilon_r \epsilon_0 d\theta \int_0^{l_t} dl \int_{r_c}^{r_o} \frac{r}{dr} = \frac{\epsilon_r \epsilon_0 l_t}{\int_{r_c}^{r_o} \frac{dr}{r}} d\theta = \frac{\epsilon_r \epsilon_0 l_t}{\ln \frac{r_o}{r_c}} d\theta. \quad (3)$$

Therefore, the capacitance per unit angle of the part of the basic cell corresponding to the insulating coatings is given by

$$\frac{dC_{ttc}}{d\theta} = \frac{dC_c}{2} = \frac{\epsilon_r \epsilon_0 l_t}{2 \ln \frac{r_o}{r_c}}. \quad (4)$$

C. Capacitance of the Air Gap

From geometrical considerations in Fig. 4, the length of the assumed paths as a function of θ is given by

$$x(\theta) = D_o(1 - \cos \theta). \quad (5)$$

The elementary surface of the wire, including coating (in the form of an elementary ring of length l_t), is

$$dS = \frac{l_t D_o}{2} d\theta \quad (6)$$

and the elementary capacitance per unit angle is

$$\frac{dC_g(\theta)}{d\theta} = \epsilon_0 \frac{l_t D_o}{2x(\theta)} = \epsilon_0 \frac{l_t D_o}{2D_o(1 - \cos \theta)} = \epsilon_0 \frac{l_t}{2(1 - \cos \theta)}. \quad (7)$$

D. Total Capacitance of the Basic Cell

The series combination of the elementary capacitances (4) and (7) is given by

$$dC_{eq}(\theta) = \frac{dC_{ttc} dC_g}{dC_{ttc} + 2dC_g} = \frac{\epsilon_0 l_t}{2} \frac{1}{1 + \frac{1}{\epsilon_r} \ln \frac{D_o}{D_c} - \cos \theta} d\theta \quad (8)$$

where $D_c = 2r_c$. Integration of (8) in the basic cell gives the overall turn-to-turn capacitance

$$C_{tt} = \epsilon_0 l_t \int_0^{\pi/6} \frac{1}{1 + \frac{1}{\epsilon_r} \ln \frac{D_o}{D_c} - \cos \theta} d\theta$$

$$= \epsilon_0 l_t \frac{2\epsilon_r \arctan \left[\frac{(-1 + \sqrt{3}) \left(2\epsilon_r + \ln \frac{D_o}{D_c} \right)}{(1 + \sqrt{3}) \sqrt{\ln \frac{D_o}{D_c} \left(2\epsilon_r + \ln \frac{D_o}{D_c} \right)}} \right]}{\sqrt{2\epsilon_r \ln \frac{D_o}{D_c} + \left(\ln \frac{D_o}{D_c} \right)^2}}. \quad (9)$$

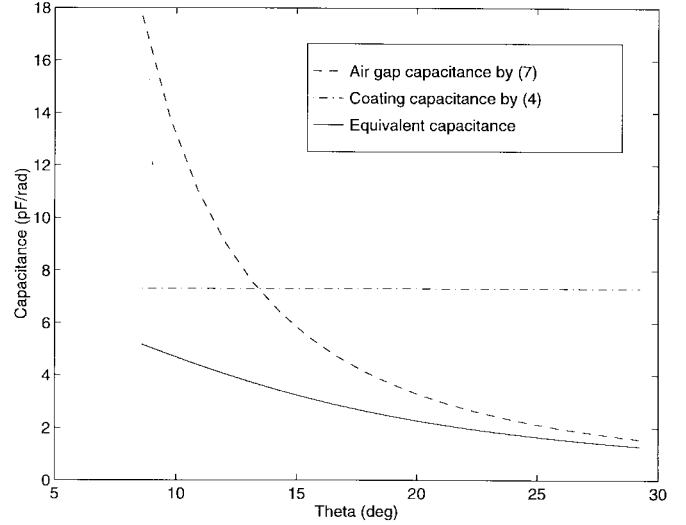


Fig. 6. Capacitances of the basic cell.

IV. TURN-TO-CORE CAPACITANCE

Equation (9) can also be used to calculate the turn-to-core and/or the turn-to-shield capacitances. Since the core is at a constant potential and located on the vertical plane of the symmetry depicted in Fig. 4, the path lengths of the electric field lines in the air gap between the turn and plane conductor are one half of the path lengths in the air gaps between two adjacent turns. The basic cell of the turn-to-core capacitance is wider than the turn-to-turn basic cell. A portion of the perimeter of the turn, which corresponds to an angle of $\pi/2$, is included in the turn-to-core basic cell, as can be seen from Fig. 2. Nevertheless, for the sake of simplicity and as a first-order approximation, we can consider the turn-to-core basic cell to be the same as the turn-to-turn basic cell. As a consequence, a similar derivation to that given in Section III yields the turn-to-core capacitance

$$C_{tc} = 2C_{tt}. \quad (10)$$

V. SIMPLIFYING APPROACH

We propose here a reasonably accurate simplifying approach that leads to an expression for the turn-to-turn capacitance that is much easier to use than (9). Fig. 6 shows plots of (7) in the dashed line, (4) in the dashed/dotted line, and (8) in the solid line. From Figs. 4 and 6, it can be seen that for $\theta = 0$, the path of the electric field \mathbf{E} in the air gap is equal to zero, and the corresponding elementary capacitance given by (7) approaches infinity. The electric field lines become longer in the air gap and the elementary capacitances smaller for increasing values of θ , whereas the elementary capacitances given by (4) remain constant all over the basic cell. Therefore, for small values of the angle θ , the elementary capacitances of the air gap are much larger than the series combinations of the elementary capacitances of the coatings. Yet, the elementary capacitance of the air gap can become much smaller than the series combination of the elementary capacitances of the coatings when θ assumes larger values. The turn-to-turn capacitance given by (9) corresponds to the area below the solid curve of

Fig. 6. The dashed and dashed/dotted curves in Fig. 6 cross each other at an angle θ^* . Thus, we can approximate the area below the solid curve with the sum of the area below the dashed/dotted curve until the crossing point at θ^* and the area below the dashed curve beyond the crossing point. This approximation is still conservative because the latter area is larger than the former one. As a consequence, the basic cell $ABCD$ of Fig. 3 can be partitioned into three parts: a middle one within $|\theta| \leq \theta^*$ and two side parts corresponding to $\theta^* < \theta \leq \pi/6$ and $-\pi/6 < \theta \leq -\theta^*$. From a computational point of view, we can replace the equivalent elementary capacitance (8) by the equivalent elementary capacitance of the coatings given by (4) for $|\theta| \leq \theta^*$ and with the elementary capacitance of the air gap given by (7) for $\theta^* < |\theta| \leq \pi/6$. As a result, we obtain the equivalent capacitance of the insulating coatings in the middle part of the basic cell

$$C_{ttc} = \frac{C_c}{2} = \frac{\epsilon_r \epsilon_0 l_t \theta^*}{\ln \frac{r_o}{r_c}}. \quad (11)$$

Furthermore, integration of (7) in the side parts of the basic cell corresponding to $\theta^* < |\theta| \leq \pi/6$ yields

$$\begin{aligned} C_{ttg} &= 2 \int_{\theta^*}^{\pi/6} \frac{\epsilon_0 l_t}{2(1 - \cos \theta)} d\theta = \epsilon_0 l_t \int_{\theta^*}^{\pi/6} \frac{1}{1 - \cos \theta} d\theta \\ &= \epsilon_0 l_t \left[\cot \left(\frac{\theta^*}{2} \right) - \cot \left(\frac{\pi}{12} \right) \right]. \end{aligned} \quad (12)$$

The angle θ^* corresponding to the crossing point in Fig. 6 can be obtained by equating (4) and (7)

$$\frac{\epsilon_r}{\ln \frac{D_o}{D_c}} = \frac{1}{1 - \cos \theta^*} \quad (13)$$

where D_c is the diameter of the conductor (excluding the insulator). Rearrangement of this equation yields

$$\theta^* = \arccos \left(1 - \frac{\ln \frac{D_o}{D_c}}{\epsilon_r} \right). \quad (14)$$

The total capacitance of the basic cell equals the parallel combination of the capacitances of the parts into which the basic cell has been subdivided

$$C_{tt} = C_{ttc} + C_{ttg} = \epsilon_0 l_t \left[\frac{\epsilon_r \theta^*}{\ln \frac{D_o}{D_c}} + \cot \left(\frac{\theta^*}{2} \right) - \cot \left(\frac{\pi}{12} \right) \right] \quad (15)$$

where θ^* is given by (14).

VI. OVERALL STRAY CAPACITANCE

In order to determine the stray capacitance of a winding, as depicted in Fig. 1, one can use the values of the turn-to-turn capacitance C_{tt} and the turn-to-core capacitance C_{tc} to calculate the equivalent layer-to-layer and layer-to-core

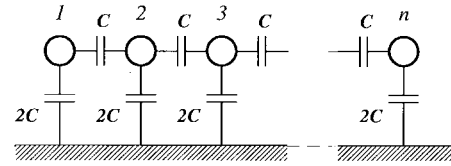


Fig. 7. Lumped capacitor network for a single-layer coil with a conductive core.

capacitances of multiple-layer coils, as described in [7]. Alternatively, a network consisting of lumped capacitors can be solved. In fact, in the high-frequency range, the reactance of the shunt capacitances between turns C_{tt} is much lower than the impedance of the RLM branches, which can be considered in a more detailed model of the winding. In this approach and in view of the high-frequency applications, the inductances and resistances of each turn are neglected (i.e., they are treated as open circuits), and a capacitor network is assumed as the equivalent circuit for the calculation of the overall stray capacitance of coils [13]. This approach is not adequate at lower frequencies, where the inductive effects still dominate.

A network of lumped capacitors obtained for a single-layer coil wound on a conductive core is shown in Fig. 7. The simplest case concerns a coreless single-layer winding of n turns. In this case, the total stray capacitance of the coil is given by the equivalent capacitance of the $n - 1$ turn-to-turn capacitances in series

$$C_s = \frac{C_{tt}}{n - 1}. \quad (16)$$

Some of the assumptions made in the previous sections are not well satisfied in this case, and, therefore, the accuracy of (16) is not always very good.

A. Single-Layer Coil with a Conductive Core

For a single-layer coil consisting of n turns wound on a conductive core, the lumped capacitor network depicted in Fig. 6 must be solved. In Fig. 6, the turns are not to the scale. They are reduced in size in order to show the capacitances between them and the core. The conducting core (or shield) can be regarded as a single node, where all the turn-to-core (or turn-to-shield) capacitances are connected, and the symmetries of the circuit can be exploited.

For coils consisting of an even number of turns, we first consider the two turns in the middle of the coil. For these turns, $n = 2$, and the network consists of the capacitance between turns 1 and 2, C_{12} , in parallel with the series combination of the turn-to-core capacitances C_{1c} and C_{2c} . Since $C_{1c} = C_{2c} = 2C_{tt}$, the equivalent capacitance of the two turns is given by $C_s = C_{tt} + 2C_{tt}/2 = 2C_{tt}$.

For an odd number of turns, we first consider the three turns in the middle of the winding. The equivalent capacitance of the capacitor network related to $n = 3$ can be calculated by splitting C_{2c} into two halves, as depicted in Fig. 8, and applying the Δ/Y transformations. The result is $C_{tt}/2 + C_{tc}/2 = C_{tt}/2 + 2C_{tt}/2 = 3C_{tt}/2$. This result can also be obtained through the observation that C_{2c} has no

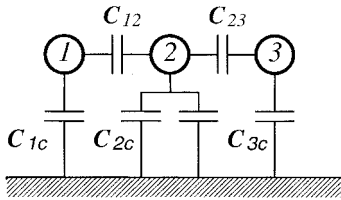


Fig. 8. Capacitances between three turns wound on a conductive core.

influence on the equivalent capacitance because of symmetry. In order to obtain the overall capacitance of coils consisting of four or five turns, we can add one more turn at each side of the two-turn or three-turn coils. The overall capacitance is equal to the capacitance of previous arrangements in series with two more turn-to-turn capacitances and in parallel with the series combination of two more turn-to-core capacitances. For $n = 4$:

$$C_s(4) = \frac{C_{tt}C_s(2)}{2C_s(2) + C_{tt}} + C_{tt} = \frac{7}{5} \times C_{tt}, \quad (17)$$

For $n = 5$:

$$C_s(5) = \frac{C_{tt}C_s(3)}{2C_s(3) + C_{tt}} + C_{tt} = \frac{11}{8} \times C_{tt}. \quad (18)$$

Adding one more turn to both sides once at a time, we can calculate the stray capacitance of coils consisting of any number of turns. Thus, for a coil consisting of n turns, we have

$$C_s(n) = \frac{C_{tt}}{2 + \frac{C_{tt}}{C_s(n-2)}} + C_{tt} \quad (19)$$

where $C_s(n-2)$ is the stray capacitance of the coil consisting of $n-2$ turns. It can be seen that the values calculated from (19) for an increasing number of turns constitute a sequence that converges very rapidly to

$$C_s \cong 1.366C_{tt}, \quad \text{for } n \geq 10. \quad (20)$$

B. Two-Layer Coreless Coil

Using a similar approach to that described in the previous subsection, we can obtain the stray capacitance for a two-layer coreless coil. Also, in this case, under the assumptions that the second layer has only one turn less than the first and it is wound in the opposite direction, a sequence of capacitances is obtained corresponding to increasing numbers of turns. The terms of the sequence converge very rapidly to

$$C_s \cong 1.618C_{tt}, \quad \text{for } n \geq 10, \quad (21)$$

C. Two-Layer Coil with a Conductive Core and Three-Layer Coil

Under the previous assumptions and when a conductive core is also present, the overall stray capacitance of a coil of n turns are in a sequence that converge to

$$C_s \cong 1.83C_{tt}, \quad \text{for } n \geq 10, \quad (22)$$

It can be seen that two-layer coils are affected by a higher stray capacitance than single-layer coils. They are also affected by

a higher resistance at high-frequency operation. Thus, using two-layer coils is not a good practice for inductors designed for high-frequency operation. The overall stray capacitance of coils with three layers decreases, but the solution of the lumped capacitor network becomes more complicated. For a three-layer coreless coil with a number of turns $n > 10$, as depicted in Fig. 2, a sequence was calculated that converges to

$$C_s \cong 0.5733C_{tt}. \quad (23)$$

It can be seen that the stray capacitance of three-layer coils is smaller than the stray capacitance of two-layer coils. But the proximity effect increases as the number of layers increases. Therefore, single-layer inductors should be used at high frequencies.

VII. COMPARISON OF PREDICTED AND MEASURED RESULTS

The results given by the proposed method have been compared with those measured for several inductors. An illustrative example is given below for a single-layer winding inductor with a powder iron core. The coil had 95 circular turns of $D_t = 14.3$ -mm diameter. Hence, the turn length was $l_t = \pi D_t = \pi \times 14.3 = 44.925$ mm. The wire had an outer diameter $D_o = 0.495$ mm with an inner diameter of the conductor $D_c = 0.45$ mm. The coating thickness was, therefore, $s = 0.0225$ mm. The dielectric constant of the coating material used for the nonimpregnated coil was $\epsilon_r = 3.5$. Therefore, using (14), (15), and (20), one obtains $\theta^* = 0.2339$ rad = 13.4° , $C_{tt} = 5.318$ pF, and $C_s = 7.26$ pF. Using this value and the inductance $L = 75.1$ μ H, the self-resonant frequency of the inductor can be predicted as $f_r = 1/(2\pi\sqrt{LC}) = 6.8$ MHz.

The same inductor was measured with a HP4194A impedance/gain-phase analyzer. The inductance measured at a frequency of 100 Hz was $L = 75.1$ μ H. The measured self-resonant frequency was $f_r = 6.2$ MHz. Hence, the total stray capacitance can be found as $C_s = 8.77$ pF. The error of determining the first self-resonant frequency f_r was 9.68%. From this result the error of determining the self-capacitance was -17.2% .

Using the more complicated expression (9), one obtains

$$C_{tt} = 8.85 \times 10^{-12} \times \pi \times 14.3 \times 10^{-3} \times \int_0^{\pi/6} \frac{1}{1 + \frac{1}{3.5} \ln \frac{0.495}{0.45} - \cos \theta} d\theta = 3.934 \text{ pF}. \quad (24)$$

It can be seen that the turn-to-turn capacitance predicted by this equation is lower than that predicted by (15). This result is consistent with the approximation introduced for deriving (15).

VIII. CONCLUSIONS

A method for predicting the stray capacitance of inductor windings has been proposed herein. A simple expression for the self-capacitance has been derived. A pocket calculator can be used to calculate the self-capacitance. The self-capacitance decreases with increasing thickness of the insulating coatings

of the conductors. The proposed approach is suitable for predicting the self-resonant frequency of inductors for both single- and multiple-layer windings. Physical insight into the influence of the number of turns and layers on the overall equivalent capacitance is provided.

New contributions of this work are as follows.

- 1) A new method for calculating the stray capacitance of inductors is shown.
- 2) Both single- and multiple-layer windings are considered.
- 3) The model is simple, accurate, and reliable for the simulation and design of inductors operated at high frequencies.

REFERENCES

- [1] P. L. Dowell, "Effects of eddy currents in transformer windings," *Proc. Inst. Elect. Eng.*, vol. 113, no. 8, pp. 1287–1394, 1966.
- [2] W. M. Flanagan, *Handbook of Transformer Applications*. New York: McGraw-Hill, 1986.
- [3] N. R. Grossner, *Transformers for Electronic Circuits*, 2nd ed. New York: McGraw-Hill, 1983.
- [4] M. K. Jutty, V. Swaminathan, and M. K. Kazimierczuk, "Frequency characteristics of ferrite core inductors," in *Proc. IEEE Electrical Manufacturing and Coil Winding Symp.*, Chicago, IL, 1993, pp. 369–372.
- [5] J. Jongsma, "High frequency ferrite power transformer and choke design—Part 3: Transformer winding design," Philips Technical, The Netherlands, 1986.
- [6] M. Bartoli, A. Reatti, and M. K. Kazimierczuk, "Modeling of iron-powder inductors at high frequencies," in *Proc. IEEE Industry Applications Conf.*, Denver, CO, 1994, pp. 1225–1232.
- [7] E. C. Snelling, *Soft Ferrites, Properties and Applications*. London, U.K.: ILIFFE Books, 1969.
- [8] W. T. Duerdoth, "Equivalent capacitances of transformer windings," *Wireless Eng.*, vol. 23, pp. 161–167, June 1946.
- [9] D. Maurice and R. H. Minns, "Very-wide-band radio frequency transformers," *Wireless Eng.*, vol. 24, pts. I–II, p. 168, p. 209, June 1947.
- [10] K. A. Macfadian, *Small Transformers and Inductors*. London, U.K.: Chapman and Hall, 1953.
- [11] H. Zuhrt, "Einfache Näherungsformeln für die Eigenkapazität Mehrlagiger-Spulen," *Elektrotech. Z.*, vol. 55, p. 662, 1934.
- [12] R. G. Medhurst, "H. F. resistance and self-capacitance of single-layer solenoids," *Wireless Eng.*, vol. 24, pp. 35–43, Feb. 1947 and pp. 80–92, Mar. 1946.
- [13] M. Kostenko and L. Piotrovsky, *Electrical Machines*, vol. 1. Moscow, Russia: Mir, 1968.



Antonio Massarini received the *Laurea* degree in nuclear engineering and the Ph.D. degree in electrical engineering from the University of Bologna, Bologna, Italy, in 1987 and 1992, respectively.

Since 1993, he has been with the Department of Engineering Sciences, Faculty of Engineering, University of Modena, Modena, Italy, as a Teaching and Research Assistant. He also works with the Electrical Engineering Department, University of Bologna, and was a Visiting Professor with the Department of Electrical Engineering, Wright State University, Dayton, OH. His research interests include MHD flow simulation, switched network simulation, magnetics, numerical methods for circuit analysis and design, and switching-power-converter simulation and design.

Marian K. Kazimierczuk (M'91–SM'91) received the M.S., Ph.D., and D.Sci. degrees in electronics engineering from the Department of Electronics, Technical University of Warsaw, Warsaw, Poland, in 1971, and 1978, and 1984, respectively.

He was a Teaching and Research Assistant from 1972 to 1978 and an Assistant Professor from 1978 to 1984 with the Department of Electronics, Institute of Radio Electronics, Technical University of Warsaw. In 1984, he was a Project Engineer for Design Automation, Inc., Lexington, MA. From 1984 to 1985, he was a Visiting Professor with the Department of Electrical Engineering, Virginia Polytechnic Institute and State University, Blacksburg. Since 1985, he has been with the Department of Electrical Engineering, Wright State University, Dayton, OH, where he is currently a Professor. His research interests are in resonant and PWM dc/dc power converters, dc/ac inverters, high-frequency rectifiers, electronic ballasts, magnetics, power semiconductor devices, and high-frequency high-efficiency power-tuned amplifiers. He is the coauthor of the book *Resonant Power Converters* (New York: Wiley, 1995). He has published more than 190 technical papers, with more than 60 appearing in various IEEE Transactions and Journals.

Dr. Kazimierczuk received the IEEE Harrell V. Noble Award in 1991 for his contributions to the fields of aerospace, industrial, and power electronics. He is also a recipient of the 1991 Presidential Award for Faculty Excellence in Research, 1993 College Teaching Award, 1995 Presidential Award for Outstanding Faculty Member, and Brage Golding Distinguished Professor of Research Award from Wright State University. He was an Associate Editor of the IEEE TRANSACTIONS ON CIRCUITS AND SYSTEMS I and serves as an Associate Editor for the *Journal of Circuits, Systems, and Computers*. He is a Member of the Superconductivity Committee of the IEEE Power Electronics Society and Tau Beta Pi.